

# Experimental and Theoretical Insights Regarding the Cycloaddition Reaction of Carbohydrate-Based 1,2-Diaza-1,3-butadienes and Acrylonitrile. A Model Case for the Behavior of Chiral Azoalkenes and Unsymmetric Olefins<sup>†</sup>

Martín Avalos, Reyes Babiano, Pedro Cintas, Fernando R. Clemente, Ruth Gordillo, José L. Jiménez, and Juan C. Palacios\*

Departamento de Química Orgánica, Facultad de Ciencias, Universidad de Extremadura, E-06071Badajoz, Spain

palacios@unex.es

Received November 5, 2001

A series of carbohydrate-based tetrahydropyridazines are prepared by the hetero-Diels–Alder reaction of the chiral 1,2-diaza-1,3-butadienes **1** and **2** with acrylonitrile. Reactions are regioselective, and the observed diastereoselection is consistent with a preferred attack to the *Re* face of the heterodiene unit, as the chiral sugar placed at C4 does largely protect the opposite *Si* face. The stereochemistry of the major cycloadduct **4** has been firmly established by an X-ray crystallographic study that, in addition, reveals a conformation placing the cyano group in axial orientation. Cycloadducts such as **9** and **11**, in which the axial cyano group and the carbohydrate moiety exhibit a *cis* relationship, undergo a facile E2 elimination that relieves the steric congestion. A detailed computational study is reported to provide better insight into the factors that influence this asymmetric cycloaddition. A DFT study (B3LYP/6-31G\*) on a reduced model does correctly predict the regiochemistry observed experimentally, while the facial diastereoselection is modeled at a semiempirical (PM3) level on the parent reagents, thereby accounting for the steric factor provided by the chiral substituent. The calculations also indicate that the axial orientation of the cyano group can be rationalized in terms of a stabilizing anomeric effect.

## Introduction

The Diels–Alder reaction (DA), by virtue of its multiple variations, constitutes the most venerable and versatile transformation in organic chemistry, often being the key step in the construction of complex skeleta and naturally occurring substances.<sup>1</sup> While the synthetic approaches are well established, an in-depth rationale of DA, hetero-DA, and related processes is still a current challenge. With the advent and growing implementation of computational methods, especially DFT and *ab initio*, in standard computers, the routine estimation of reaction pathways and transition structures have come of age, thereby replacing *a priori* models based on putative steric and electronic interactions. In this manuscript, we will draw on a selected hetero-DA cycloaddition consisting of a chiral 1,2-diaza-1,3-butadiene plus acrylonitrile to illustrate how a combined analysis of experimental and theoretical data has led to a better understanding of factors controlling regio- and stereoselectivities. These results demonstrate the influence of the key elements

involved in stereocontrol and, in particular, of a chiral element anchored to the heterodiene.

Recent papers from this laboratory have described a route to nitrogenated ring systems that involves the stereocontrolled reaction of a carbohydrate-based 1,2-diaza-1,3-butadiene acting as the heterodiene or dienophile.<sup>2,3</sup> Moreover, such homochiral butadienes can easily be prepared from commercially available sources.<sup>4</sup> To model the behavior of these systems toward unsymmetrically substituted olefins, we have chosen acrylonitrile as the  $2\pi$  component in an attempt to answer a series of emerging questions: (a) would the intermolecular cycloaddition take place with a high degree of regio- and stereoselectivity, and (b) if so, what influence would the chirogenic elements of the heterodiene have on the steric course? The present study is therefore a part of our program aimed at testing the above issues, thereby providing a plausible explanation from a theoretical viewpoint.

\* Corresponding author: Juan C. Palacios. Tel: +34-924-289380. Fax: +34-924-271149.

<sup>†</sup> Dedicated to Professor Manuel Martín-Lomas on the occasion of his 60th birthday.

(1) For comprehensive treatments of cycloaddition reactions: (a) Carruthers, W. *Cycloaddition Reactions in Organic Synthesis*; Pergamon: Oxford, 1990. (b) Fringuelli, F.; Taticchi, A. *Dienes in the Diels–Alder Reaction*; Wiley: New York, 1990. (c) *Comprehensive Organic Synthesis*; Trost, B. M., Fleming, I., Paquette, L. A., Eds.; Pergamon: Oxford, 1991; Vol. 5, pp 1–673. (d) *Advances in Cycloadditions*; Curran, D. P., Ed.; JAI Press: Greenwich, CT; 1988; Vol. 1; 1990; Vol. 2; 1993; Vol. 3; 1996; Vol. 4. (e) Tietze, L. F.; Ketschschau, G. *Top. Curr. Chem.* **1997**, *189*, 1–120.

(2) (a) Avalos, M.; Babiano, R.; Cintas, P.; Jiménez, J. L.; Molina, M. M.; Palacios, J. C.; Sánchez, J. B. *Tetrahedron Lett.* **1991**, *32*, 2513–2516. (b) Avalos, M.; Babiano, R.; Cintas, P.; Clemente, F. R.; Jiménez, J. L.; Palacios, J. C.; Sánchez, J. B. *J. Org. Chem.* **1999**, *64*, 6297–6305. (c) Avalos, M.; Babiano, R.; Cintas, P.; Clemente, F. R.; Gordillo, R.; Jiménez, J. L.; Palacios, J. C.; Raithby, P. R. *J. Org. Chem.* **2000**, *65*, 5089–5097. (d) Avalos, M.; Babiano, R.; Cintas, P.; Clemente, F. R.; Gordillo, R.; Jiménez, J. L.; Palacios, J. C. *J. Org. Chem.* **2001**, *66*, 5139–5145.

(3) For a theoretical study on the [4 + 2] cycloaddition reactions of 1,2-diaza-1,3-butadiene: Avalos, M.; Babiano, R.; Cintas, P.; Clemente, F. R.; Gordillo, R.; Jiménez, J. L.; Palacios, J. C. *J. Org. Chem.* **2000**, *65*, 8251–8259.

(4) Avalos, M.; Babiano, R.; Cintas, P.; Jiménez, J. L.; Palacios, J. C.; Sánchez, J. B. *Tetrahedron: Asymmetry* **1995**, *6*, 945–956.

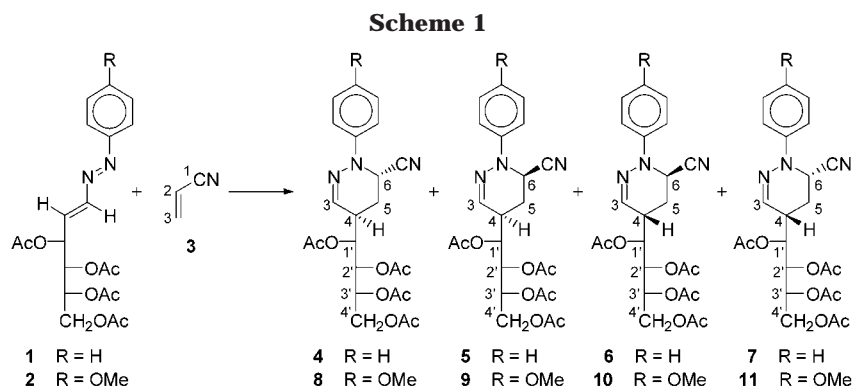


**Table 1. Isolated Yields and  $^1\text{H}$  NMR Ratios of Products for the Crude Reaction Mixtures of 1 or 2 with 3**

compound	yield (%) <sup>a,b</sup>	composition (%) <sup>c</sup>	diastereomeric proportion <sup>c</sup>	exo/endo ratio <sup>c</sup>
1	24	30		
4	20 (26)	31	5.7	1.2:1
5	16 (21)	27	4.9	
6	3 (4)	6	1.0	0.8:1
7	3 (3)	7	1.2	
2	28	31		
8	15 (21)	31	5.9	1.2:1
9	13 (18)	25	4.8	
10	3 (4)	8	1.5	1.5:1
11	5 (7)	5	1.0	

<sup>a</sup> These values refer to isolated yields. <sup>b</sup> Corrected yields after subtracting the recovered heterodiene are given in parentheses. <sup>c</sup> Determined by  $^1\text{H}$  NMR integration on the crude samples.

## Results and Discussion

**Syntheses.** The [4 + 2] cycloaddition of **1**<sup>4</sup> with neat acrylonitrile (**3**) was first examined. This transformation proceeded slowly at room temperature and, after a week, TLC analysis (benzene–diethyl ether 1:1) evidenced the formation of four products having  $R_f$  values of 0.6, 0.5, 0.4, and 0.3. Under these conditions, the reaction was unpractical because a conversion lesser than 50% was observed after 6 months at room temperature. Attempts to accelerate this transformation at reflux also resulted in a greater decomposition. Alternative heating with a microwave oven proved to be the optimal choice, as it promoted the expected cycloaddition without the formation of side products and ~70% conversion within 24 h (Table 1). Cycloadducts **4** ( $R_f = 0.6$ ), **5** ( $R_f = 0.4$ ), **6** ( $R_f = 0.5$ ), and **7** ( $R_f = 0.3$ ) were separated by silica gel chromatography (diethyl ether–petroleum ether 1:1), although only the former could be isolated in crystalline form (Scheme 1).

Both crystallographic and spectroscopic data (vide infra) suggest that this cycloaddition proceeds with complete regioselectivity to afford diastereomeric 4-(1',2',3',4'-tetra-*O*-acetyl-D-*arabino*-tetritol-1'-yl)-6-cyano-1-phenyl-1,4,5,6-tetrahydropyridazines (**4–7**). No signs

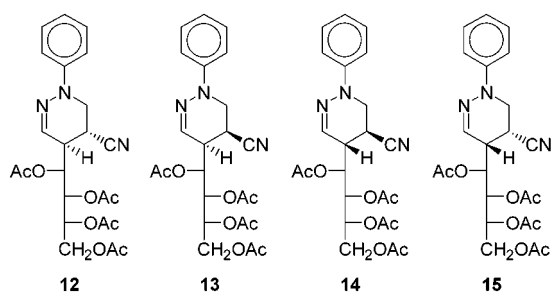
of the alternative 5-cyano derivatives (**12–15**) could be detected in the crude reaction mixture.

Similar results were obtained upon heating a sample of 1,2-diaza-1,3-butadiene **2**<sup>4</sup> with acrylonitrile (Scheme 1). The resulting cycloadducts **8**, **9**, and **11** ( $R_f = 0.6$ , 0.4, and 0.3, respectively, benzene–diethyl ether 1:1) could be isolated as crystalline materials, while **10** was isolated as a yellowish oil.

**Structural Elucidation.** Structural assignments of the above-mentioned cycloadducts were made on the basis of their spectral properties. In all cases studied, the similarity of the  $^1\text{H}$  and  $^{13}\text{C}$  chemical shifts fully agree with the formation of 6-cyano-substituted 1,4,5,6-tetrahydropyridazines. The stereochemical assignment of cycloadduct **4** was unambiguously determined by X-ray crystallography and reported elsewhere,<sup>5</sup> thereby establishing the configuration at the newly created chiral centers as 4*R*,6*S*. Remarkable features emerging from this single-crystal analysis are the existence of a conformation intermediate between a boat and a twist boat for the heterocyclic ring with the cyano group adopting an axial disposition, while both the aromatic ring and the sugar backbone prefer to be equatorial.

In solution, these cycloadducts exhibited an UV band in the range 240–230 nm consistent with the presence of an aromatic moiety and another band at 275–265 nm, the latter presumably associated to the  $\pi-\pi^*$  transition of the azomethine bond. It is also interesting to note that the adducts showed a weak IR band at  $\sim 1610\text{ cm}^{-1}$  for a C=N, suggesting the formation of [4 + 2] cycloadducts, whereas very weak or no band could be observed for the cyano group.<sup>6</sup> However, the presence of this functional group is clearly evidenced by the signal at  $\delta \sim 116\text{ ppm}$  in the  $^{13}\text{C}$  NMR spectra. NMR data for compounds **4–11** led us to determine the conformational behavior of these substances in solution (Tables 2 and 3). The heterocyclic moiety adopts a half-chair conformation (Figure 1) as expected for six-membered rings having an endocyclic double bond.<sup>7</sup>

For compound **4**, the magnitude of  $J_{4,5\text{ax}}$  (13.0 Hz) suggest an antiperiplanar arrangement between H4 and H5ax which should be in an axial or quasi-axial orienta-



(5) Diáñez, M. J.; Estrada, M. D.; López-Castro, A.; Pérez-Garrido, S. Z. *Kristallogr.* **1995**, *210*, 885–886.

(6) (a) This behavior is often encountered for cyano groups bearing electron-withdrawing substituents at C $\alpha$ . Intensities of C=N bonds show a marked variation, from very strong to undetectable; see: Bellamy, L. J. *The Infrared Spectra of Complex Molecules*, 3rd ed.; Chapman and Hall: New York, 1975; Vol. 1, p 297. (b) An explanation may be found in Nakanishi, K. *Infrared Absorption Spectroscopy*; Holden-Day, Inc.: San Francisco, 1977; p 64.

(7) Stoddart, J. F. *Stereochemistry of Carbohydrates*; Wiley: New York, 1971; p 93.

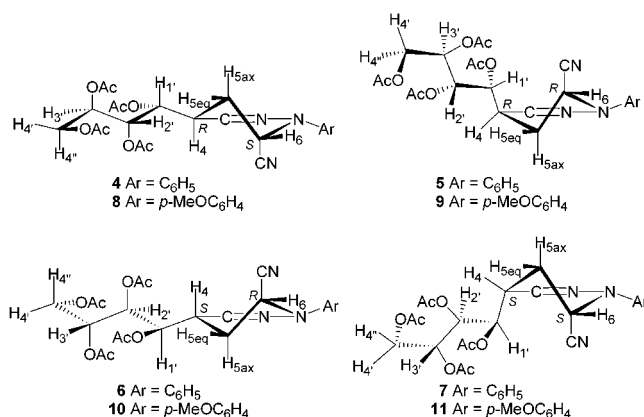
**Table 2. Selected <sup>1</sup>H NMR Chemical Shifts for Cycloadducts 4–11**

	H-3	H-4	H-5ax	H-5eq	H-6	H-1'
<b>4</b>	6.64	2.81	2.04	2.51	4.88	5.25
<b>5</b>	6.84		2.39	2.50	4.82	5.75
<b>6</b>	6.89	2.96	2.28	2.36	4.92	5.37
<b>7</b>	7.10	2.09	1.53	1.96	3.87	5.80
<b>8</b>	6.63	2.80	2.11	2.48	4.76	5.24
<b>9</b>	6.82	2.38		2.45	4.63	5.68
<b>10</b>	6.86	2.94		2.34	4.77	5.36
<b>11</b>	7.06	2.55	2.43	2.36	4.55	5.63

**Table 3. HH Coupling Constants of the Tetrahydropyridazine Unit for Cycloadducts 4–11<sup>a</sup>**

	$J_{3,4}$	$J_{3,5eq}$	$J_{4,5ax}$	$J_{4,5eq}$	$J_{5ax,5eq}$	$J_{5ax,6}$	$J_{5eq,6}$	$J_{1',4}$
<b>4</b>	1.4	1.8	13.0	6.0	13.4	4.4	2.9	9.0
<b>5</b>	<2.0	<1.5	—	6.9	12.1	4.1	3.3	8.6
<b>6</b>	1.1	1.3	12.6	6.5	12.7	4.2	3.2	6.9
<b>7</b>	<2.5	<2.0	8.6	2.6	14.4	5.5	3.1	7.0
<b>8</b>	1.2	2.3	12.2	6.2	12.9	4.4	2.5	9.0
<b>9</b>	2.5	—	4.4	—	—	4.5	—	9.6
<b>10</b>	<2.0	—	9.6	—	—	3.5	—	6.9
<b>11</b>	2.0	1.5	8.2	4.1	14.0	4.7	4.5	7.1

<sup>a</sup> These values were measured on the corresponding decoupled spectra.

**Figure 1.** Conformations for cycloadducts 4–7 and 8–11 as deduced from NMR data.

tion, whereas the coupling constants of  $J_{4,5eq}$  (6.0 Hz),  $J_{5eq,6}$  (2.9 Hz), and  $J_{5ax,6}$  (4.4 Hz) indicate that H5eq and H6 are in an equatorial disposition. Accordingly, such values suggest both an axial disposition for the cyano group and a preferential  ${}^5H_6$  conformation for the heteroatomic ring of tetrahydropyridazine. The latter conformation is also evidenced by the W-shaped arrangement of the bonds between the azomethine proton and the equatorial hydrogen located at C5, leading to a distinctive  ${}^4J_{H,H}$  coupling ( $J_{3,5eq} = 1.4$  Hz). It is equally noteworthy in fact that, like in the crystallographic study, the cyano group is axial, thereby suggesting a pseudoanomeric effect.<sup>8</sup> The analysis of the coupling constants of the <sup>1</sup>H NMR spectra of 5–11 led to the same conclusions.

The HH coupling constant between H4 and H1' of 4 ( $J_{1',4} = 9.0$  Hz) reflects the antiperiplanar disposition of these protons located at the pyridazine moiety and the acyclic sugar chain, respectively. A further analysis of

the remaining sugar protons suggests that the *P* conformation<sup>9</sup> (a zigzag arrangement) should be the favorable conformation for the tetraacetoxybutyl chain.

The chemical shifts in the <sup>1</sup>H and <sup>13</sup>C NMR spectra as well as the HH coupling constants of the adduct 8 are comparable to those observed for compound 4, thus indicating that the same [4 + 2] cycloadduct was consistently obtained. In addition, this could also be corroborated on the basis of the fragmentation pattern observed by recording their high-resolution mass spectra.

After 4 and 8, the most abundant diastereomers are 5 and 9 ( $R_f = 0.4$ ). It was difficult on the basis of NMR data to determine with absolute certainty which of the adducts we had obtained, albeit due to their spectroscopic similarity with 4 and 8 and positive optical rotations, we have assigned them the opposite configuration at C6 (see next section).

The less abundant isomers ( $R_f = 0.5$ ) have been obtained by further purification of the major isomers 4 and 8 (having 4*R*,6*S* configurations) using preparative TLC (diethyl ether–petroleum ether 1:1) and attributed to the diastereomers 6 and 10 with 4*S*,6*R* configurations, which exhibit negative optical rotations. The 4*S*,6*R* configuration assigned to 6 and 10 indicate an enantiomeric relationship with 4 and 8, respectively, in the heterocyclic moiety which is evidenced by similar chemical shifts and coupling constants (Tables 2 and 3). Thus, the 1,3-diaxial disposition between the C≡N group and H-4 in 4, 8 and 6, 10 is responsible for the deshielding experienced by H-4 ( $\delta \sim 2.8$ –2.9 ppm) with respect to that proton in 5, 9 and 7, 11 ( $\delta \sim 2.0$ –2.5 ppm). In addition, the  ${}^6H_5$  conformation of the heterocyclic ring in 6, 10 is in agreement with the high value of  $J_{4,5ax}$  ( $\sim 13$  Hz) which indicate the antiperiplanar disposition for H-4 and H-5ax (Figure 1). Finally, we have attributed a 4*S*,6*S* configuration to the minor diastereomers with  $R_f = 0.3$ , 7 and 11, which show similar chemical shifts to those of 5 and 9 (Table 2), respectively.

**Absolute Configuration at the Newly Created Chiral Centers.** In a previous study<sup>2b</sup> concerning the cycloaddition of these chiral azoalkenes with diethyl azodicarboxylate the major isomer was found to be that in which the cycloaddition had occurred on the *Re* face of the heterodiene. If the present cycloaddition had occurred via the same steric course one would have expected the formation of (4*R*)-configured cycloadducts (4, 8 and 5, 9) as major isomers (see next section). The solid-state structure of 4, determined by X-ray crystallography, reveals that this cycloadduct possesses 4*R*,6*S* configurations, which can analogously be attributed to 8. The other major diastereomers 5 and 9 should therefore present 4*R*,6*R* configurations. This assumption fully agrees with the circular dichroism (CD) spectra of compounds 8 and 9 (Figure 2). The spectra of both products show a negative Cotton effect at  $\sim 230$ –240 nm and a positive one at  $\sim 270$  nm (associated with the  $\pi$ – $\pi^*$  transition of the azomethine bond in the UV spectra). Similar CD spectra were found in structurally related tetrahydrotetrazines with absolute *R* configuration.<sup>2b</sup> As a consequence, the less abundant diastereomers should exhibit the *S* configuration at C-4. The assignment of 6*R*–

(8) (a) Pinto, B. M.; Leung, R. Y. N. In *The Anomeric Effect and Associated Stereoelectronic Effects*; Thatcher, G. R. J., Ed.; ACS Symposium Series 539; American Chemical Society: Washington, DC, 1993; pp 126–155. (b) Juaristi, E.; Cuevas, G. *The Anomeric Effect*; CRC Press: Boca Raton, FL, 1995.

(9) (a) El Khadem, H. S.; Horton, D.; Page, T. F. *J. Org. Chem.* **1968**, *33*, 734–740. (b) Lyle, G. G.; Piazza, M. J. *J. Org. Chem.* **1968**, *33*, 2478–2484. (c) Horton, D.; Wander, J. D. *Carbohydr. Res.* **1970**, *13*, 33–47.

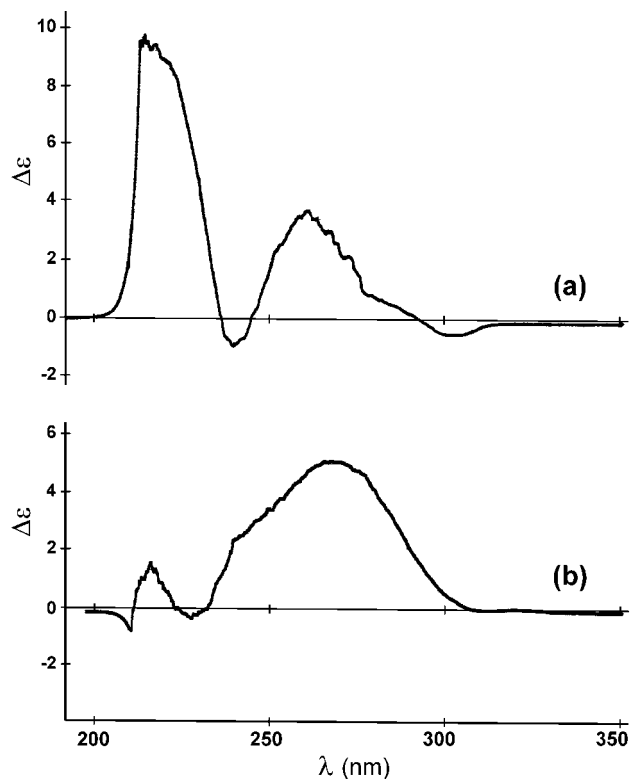


**Figure 2.** Circular dichroism spectra of diastereoisomers: (a) **8** and (b) **9** in EtOH solution.

configuration to **6**, **10** and  $6S$  to **7**, **11** is based on the similarity of spectroscopic data of their heterocyclic fragment with those of **4**, **8** and **5**, **9**, respectively.

In an attempt to correlate the molecular rotation with the configuration at that chiral center, we also envisioned that a dextrorotatory magnitude could be coupled with  $4R$ -configured heterocycles (cases of **4**, **5**, **8**, and **9**), while the opposite  $4S$  configuration would lead to levorotatory derivatives. This argument reflects the well-known empirical rules of isorotation<sup>10</sup> and van't Hoff's principle of optical superposition,<sup>11</sup> which state that individual chiral centers in a chiral substance make independent contributions to the molecular rotation. With these premises, the optical rotation observed for compound **8** will be made up of the algebraic sum of the rotatory contributions from all the stereogenic centers, i.e.,  $4R$  ( $R$ ),  $6S$  ( $S$ ), and all the carbon atoms of the acyclic carbohydrate ( $C$ ):

$$[\alpha]_D = +191^\circ = R + S + C \quad (1)$$

Compound **9**, being dextrorotatory as well, differs only by the configuration at C6 ( $R' = -S'$ ):

$$[\alpha]_D = +152^\circ = R + R' + C = R - S' + C \quad (2)$$

By the same reasoning, compounds **10** and **11**, which are levorotatory and should present  $4S$  configurations, will also have opposite configuration at C6:

$$[\alpha]_D = -98^\circ = S + R' + C = -R - S' + C \quad (3)$$

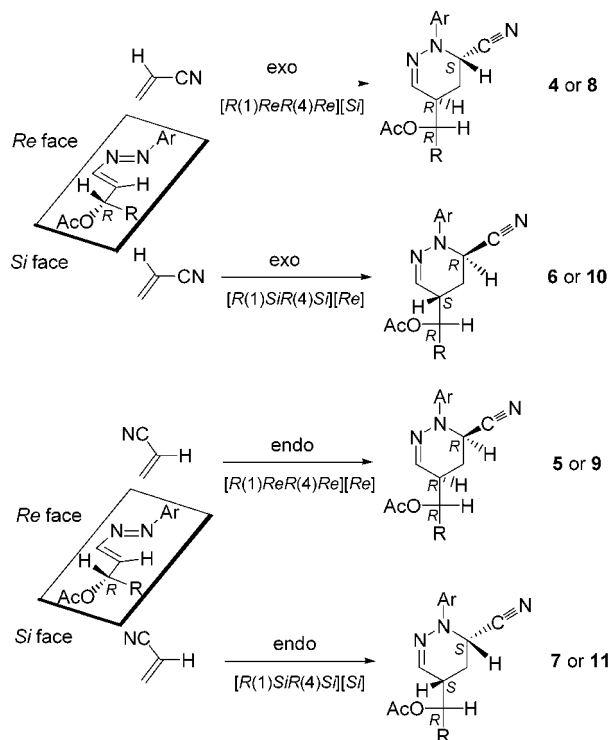
$$[\alpha]_D = -76^\circ = S + S' + C = -R + S' + C \quad (4)$$

The above set of four equations can be solved to obtain the average values of such chiral contributions as follows:  $R = +129.3^\circ$ ,  $S' = +15.3^\circ$ ,  $C = +42.3^\circ$ . These

**Table 4.** Optical Rotations for Cycloadducts **8–11**

	absolute configuration		[ $\alpha$ ] <sub>D</sub> , deg	
	C-4	C-6	observed	calculated
<b>8</b>	<i>R</i>	<i>S</i>	+191	+187
<b>9</b>	<i>R</i>	<i>R</i>	+152	+156
<b>10</b>	<i>S</i>	<i>R</i>	-98	-102
<b>11</b>	<i>S</i>	<i>S</i>	-76	-72

**Scheme 2.** Facial Selectivity for the Hetero-DA Cycloaddition of 1,2-Diaza-1,3-butadienes with Acrylonitrile (**3**)



magnitudes can now be used to evaluate the calculated versus observed molecular rotations for cycloadducts **8** and **11** (Table 4).

Because the magnitude of the  $R$  contribution is much greater than the sum of  $S' + C$ , the sign of the molecular rotation is governed by the absolute configuration at C4, in which positive values agree consistently with  $4R$ -configured tetrahydropyridazines. This reasoning can likewise be made in the cases of adducts **4–7** leading to similar conclusions. As a concluding corollary, in the set of diastereomers obtained through the cycloaddition reaction of 1,2-diaza-1,3-butadienes with acrylonitrile, a positive value of the optical rotation indicates an  $R$ -configuration at C4, whereas a negative value agrees with an  $S$ -configuration.

**Diastereofacial Selection.** As expected, the stereochemical outcome of these hetero-DA reactions arises from endo and exo attacks of acrylonitrile to both prochiral faces of the 1,2-diaza-1,3-butadiene derivative. We will henceforth denote *Re*- and *Si*-faces of the heterodiene in *s-cis* conformation, the ones in which all the prochiral centers are  $1Re, 2Re, 3Re, 4Re$  and  $1Si, 2Si, 3Si, 4Si$ , respectively. As depicted in Scheme 2, the most abundant diastereomers (**4**, **5** and **8**, **9**) correspond to endo and exo attacks to the *Re* face of the heterodiene. This also suggests that the configuration at the newly created stereocenter C4 ( $R$  in the above-mentioned cycloadducts)

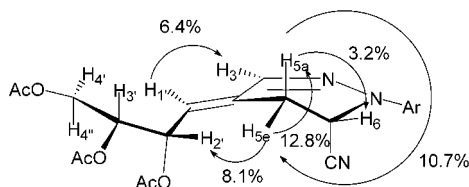
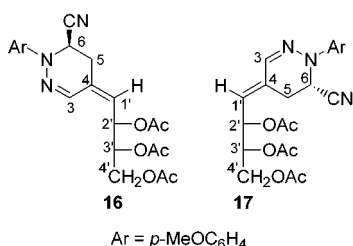


**Figure 3.** NOE enhancements observed for compound **17**.

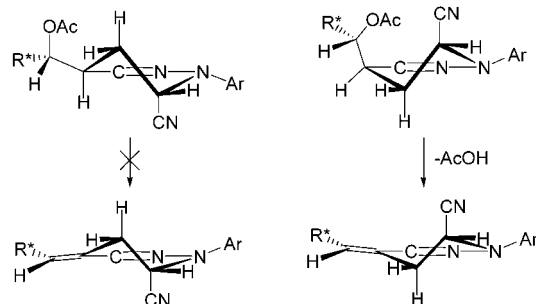
is largely dictated by the first stereocenter (*R*) of the carbohydrate framework as observed recently in related cycloaddition reactions.<sup>2b-d</sup> Since the ratios **4:5** and **8:9** are close to 1, and the same also holds for the minor isomers **6:7** and **10:11**, one may also conclude that there is no facial discrimination between the faces of acrylonitrile (vide supra, Table 1). Thus, the cycloaddition is singly diastereoselective in that the dienophile approaches preferentially to the *Re* face of the heterodiene unit.

**Formation of 1,4,5,6-Tetrahydropyridazin-4-ylidene Derivatives.** During the course of this research, it was observed that, in chloroform solution, cycloadducts **9** and **11** can be quantitatively converted to the isomeric pyridazines **16** and **17**, respectively.



The structure and stereochemistry of the latter substances, arising from **9** and **11** by loss of acetic acid, were assigned on the basis of a detailed spectroscopic analysis. Thus, compound **16** showed UV bands at 241 nm, characteristic of the aromatic ring, and 327 nm, the latter having experienced a shift to a longer wavelength than the parent compound **9** (~270 nm). This suggests the existence of a conjugated system between the C=N bond and the exocyclic double bond and hence the longer the wavelength of light this compound can absorb. The conjugation also reveals that the loss of acetic acid took place at the first stereocenter of the sugar backbone. It is also interesting to note that only three signals were observed in the <sup>13</sup>C NMR spectra for the acetate groups, and C4 and C1' resonated at ~127 ppm, a shift characteristic of olefinic carbons (for compound **16** such carbon atoms appeared at 127.2 and 126.8, respectively). The final proof rested on NOE analysis of adduct **17**, allowing an easy identification of the *E* configuration around the exocyclic double bond. As shown in Figure 3, irradiation of H1' enhances the proton H3 (6.4%), a fact that indicates the proximity between both protons and is consistent with an *E* configuration for the double bond. Irradiation of H2' enhances the equatorial proton H5eq still further (8.1%). Although it is well-known that the existence of a NOE between two protons does not, on its

### Scheme 3. Influence of the Carbohydrate Moiety on the Anti Elimination of Acetic Acid in Tetrahydropyridazines



own, give sufficient evidence that they are close,<sup>12</sup> the consideration of H2' and H5eq as nearby protons is a consequence of the antiperiplanar relationship between H1' and H2' ( $J_{1,2'} = 9.2$  Hz), and this fact should also reflect the *E* configuration of the olefinic bond. Furthermore, such a stereochemical assignment suggests that the loss of acetic acid occurred through an E2 elimination mechanism (Scheme 3). Unfortunately, a set of similar NOE experiments could not be carried out for compound **16** because its protons H1' and H2' showed very close chemical shifts. Nevertheless, if one assumes that the starting cycloadducts **9** and **11** are diastereomers bearing an enantiomeric relationship with respect to their stereocenters at the heterocyclic moiety, the same anti elimination should be expected to occur, thus implicating the *Z* configuration for the double bond of **16**.

From a stereochemical viewpoint, one additional consideration needs mention. The enantiomeric relationship between the heterocyclic stereocenters of cycloadducts **9** and **11** (and **8** and **10** as well), also implies an identical conformational behavior. The axial orientation of the cyano group imposed by the stabilizing anomeric effect places the bulky carbohydrate chain at C4 in an equatorial disposition for compounds **8** and **10**. Presumably, when the carbohydrate skeleton adopts an axial orientation (e.g. cycloadducts **9** and **11**), elimination of acetic acid greatly alleviates the steric hindrance caused by this bulky substituent, thus leading to **16** or **17** (Scheme 3).

**Theoretical Rationale.** At the outset, it was important to provide a satisfactory explanation of the regio- and stereochemical patterns observed for this hetero-DA cycloaddition. The Becke3LYP nonlocal density functional method (DFT)<sup>13,14</sup> in conjunction with a 6-31G\* basis set<sup>15</sup> was applied to all optimizations (i.e., B3LYP/6-31G\*) using the Gaussian 98 package.<sup>16</sup>

It is now well established that DFT methods often lead to transition structures comparable to other ab initio protocols at a lower computational cost. Obviously, the use of a higher level of computation also imposes the use of reduced chemical models. Previous studies have revealed the 1,2-diaza-1,3-butadiene **18** does reproduce well

(12) Derome, A. E. *Modern NMR Techniques for Chemistry Research*; Pergamon: Oxford, 1987; pp 109–111.

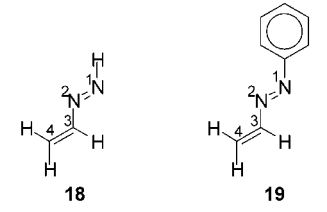
(13) (a) Parr, R. G.; Yang, W. *Density Functional Theory of Atoms and Molecules*; Oxford University Press: New York, 1989. (b) Bartolotti, L. J.; Fluchick, K. In *Reviews in Computational Chemistry*; Lipkowitz, K. B., Boyd, D. B., Eds.; VCH: New York, 1996; Vol. 7, pp 187–216.

(14) (a) Lee, C.; Yang, W.; Parr, R. G. *Phys. Rev. B* **1988**, *37*, 785–789. (b) Becke, A. D. *Phys. Rev. A* **1988**, *38*, 3098–3100. (c) Becke, A. D. *J. Chem. Phys.* **1993**, *98*, 5648–5652.

(15) Hehre, W. J.; Radom, L.; Schleyer, P. v. R.; Pople, J. A. *Ab Initio Molecular Orbital Theory*; Wiley: New York, 1986; pp 65–88.

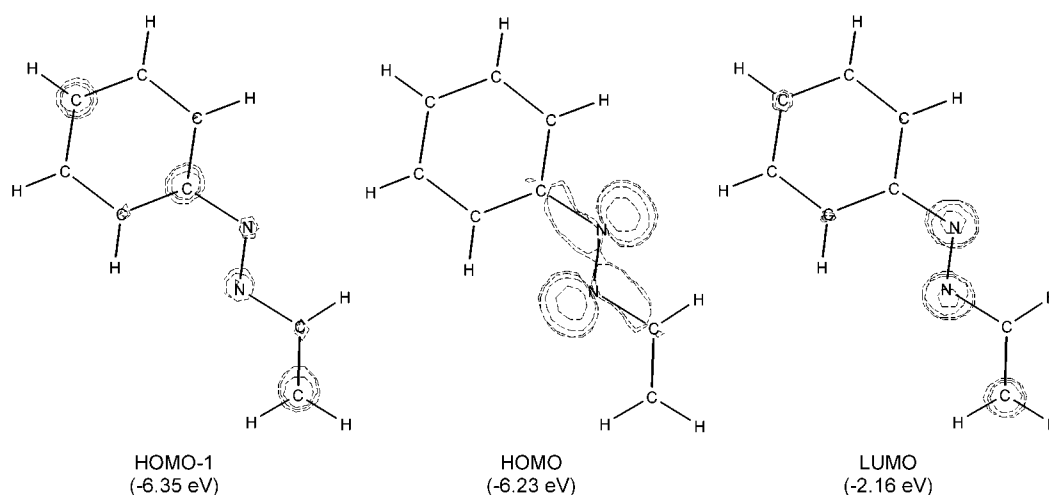
(10) (a) Pigman, W.; Horton, D. In *The Carbohydrates. Chemistry and Biochemistry*; Pigman, W., Horton, D., Eds.; Academic Press: New York, 1972; pp 45–46. (b) Reference 7, pp 152–153.

(11) Eliel, E. L.; Wilen, S. H. *Stereochemistry of Organic Compounds*; Wiley: New York, 1994; pp 1080–1081.

**Table 5.** FMO Analysis of Heterodienes **18** and **19** and Acrylonitrile (**3**)<sup>a</sup>


		<i>E</i> (eV)	<i>c</i> <sub>1</sub>		<i>c</i> <sub>2</sub>		<i>c</i> <sub>3</sub>		<i>c</i> <sub>4</sub>	
			2pz	3pz	2pz	3pz	2pz	3pz	2pz	3pz
<b>18</b>	HOMO <sup>b</sup>	-7.50	-0.28	-0.21	-0.10	-0.07	+0.35	+0.23	+0.38	+0.28
	LUMO	-1.82	+0.43	+0.43	-0.37	-0.34	-0.16	-0.18	+0.32	+0.36
<b>19</b>	HOMO <sup>b</sup>	-6.35	-0.16	-0.12	-0.21	-0.15	+0.17	+0.11	+0.26	+0.21
	LUMO	-2.16	+0.35	+0.31	-0.34	-0.31	-0.10	-0.11	+0.27	+0.30
<b>3</b>	HOMO	-7.87	-0.19	-0.12	+0.31	+0.22	+0.35	+0.25	—	—
	LUMO	-1.53	-0.18	-0.16	-0.32	-0.42	+0.41	+0.53	—	—

<sup>a</sup> *c*<sub>i</sub> = atomic coefficient for atom *i*. <sup>b</sup> HOMO-1 orbital.

**Figure 4.** Isopotential surfaces (cutoff value = 0.1) of the frontier orbitals of **19** computed at the B3LYP/6-31G\* level.

the regiochemical profile of hetero-DA reactions with ethene, methyl vinyl ether, and methyl acrylate.<sup>3</sup> Bolstered by this positive result, we have decided to test the reliability of this structural model in the present cycloaddition with acrylonitrile (**3**). In addition, the heterodiene **19**, which mimics more adequately the azoalkene moiety of experiments, has also been considered.

Calculations of frontier molecular orbital (FMO) energies and MO coefficients (Table 5) suggest that the behavior toward acrylonitrile is similar to that of **18** with methyl acrylate.<sup>3</sup> This is a case in which the HOMO–LUMO separations are equivalent and there is no major frontier orbital interaction. It should be noted that the HOMO-1 should be considered as the heterodiene HOMO, because only that frontier orbital possesses the adequate

symmetry (vide infra) to react in a hetero-DA cycloaddition. Likewise, the acrylonitrile HOMO exhibits a weak polarization, a fact that rules out a preferential regioselection, although the LUMO coefficient for C3 is higher than for C2 and hence the orbital interaction between the heterodiene HOMO and the dienophile LUMO would lead to cycloadducts substituted at C6 in agreement with our experimental results.

A further analysis of the four possible transition structures involving **18** and **3** reveals, however, that the formation of tetrahydropyridazines substituted with a cyano group at C5 will be the favored pathway, a result that disagrees with previous experiments and FMO theory. The failed prediction can be traced to a poor structural model, as **18** lacks the aromatic moiety linked to N1. Such a substituent could play an important role since both reaction partners (**18** and **3**) are electronically poor substrates, and little or no difference between the frontier orbitals should be expected in either way (normal or inverse electron demand). In contrast, an aryl group upon extending the conjugation further will increase the HOMO-1 energy, thereby promoting a normal electron demand [4 + 2] cycloaddition. With these premises, we next examined the regiochemical issue using 1-phenyl-1,2-diaza-1,3-butadiene (**19**) as heterodiene. Figure 4<sup>17</sup> depicts the isopotential surfaces of the frontier orbitals

(16) Frisch, M. J.; Trucks, G. W.; Schlegel, H. B.; Scuseria, G. E.; Robb, M. A.; Cheeseman, J. R.; Zakrzewski, V. G.; Montgomery, J. A., Jr.; Stratmann, R. E.; Burant, J. C.; Dapprich, S.; Millam, J. M.; Daniels, A. D.; Kudin, K. N.; Strain, M. C.; Farkas, O.; Tomasi, J.; Barone, V.; Cossi, M.; Cammi, R.; Mennucci, B.; Pomelli, C.; Adamo, C.; Clifford, S.; Ochterski, J.; Petersson, G. A.; Ayala, P. Y.; Cui, Q.; Morokuma, K.; Malick, D. K.; Rabuck, A. D.; Raghavachari, K.; Foresman, J. B.; Cioslowski, J.; Ortiz, J. V.; Baboul, A. G.; Stefanov, B. B.; Liu, G.; Liashenko, A.; Piskorz, P.; Komaromi, I.; Gomperts, R.; Martin, R. L.; Fox, D. J.; Keith, T.; Al-Laham, M. A.; Peng, C. Y.; Nanayakkara, A.; Gonzalez, C.; Challacombe, M.; Gill, P. M. W.; Johnson, B.; Chen, W.; Wong, M. W.; Andres, J. L.; Gonzalez, C.; Head-Gordon, M.; Replogle, E. S.; Pople, J. A. *Gaussian 98*, revision A.7; Gaussian, Inc.: Pittsburgh, PA, 1998.

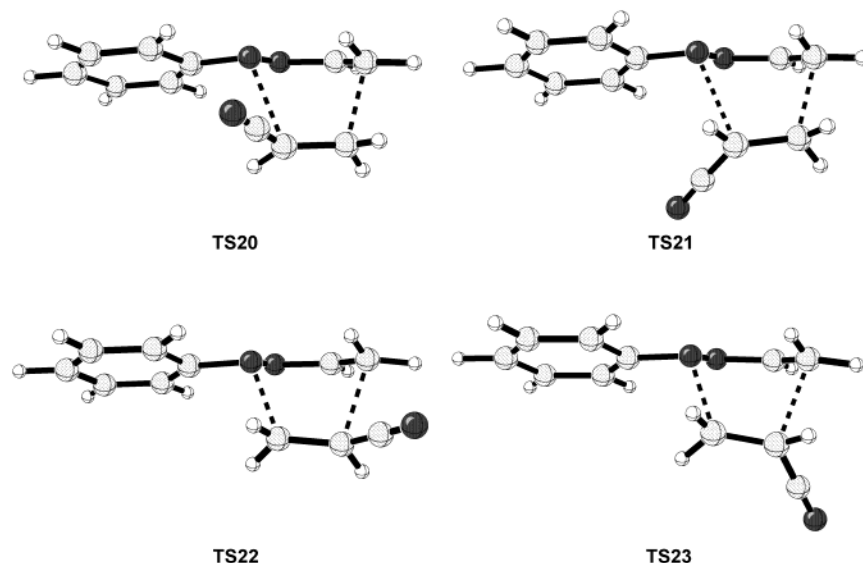


**Figure 5.** Optimized transition structures for the hetero-DA reaction of **3** and **19** at the B3LYP/6-31G\* level of theory.

of **19**. As noted previously, the standard HOMO does not have the appropriate symmetry to overlap with the LUMO of acrylonitrile, a role otherwise possible with the HOMO-1. Moreover, as a result of the extended conjugation through the  $\pi$  system, the HOMO-1 of **19** lies very close to its HOMO ( $\Delta E = 0.12$  eV), while a larger difference is encountered between the HOMO and HOMO-1 of **18** ( $\Delta E = 1.1$  eV).

Examination of the MO coefficients of the HOMO-1 of **19** clearly indicates a higher polarization (N1 < C4), and this along with the coefficients in the LUMO of **3** (C3 > C2) provide an interpretation of the exclusive regioselectivity observed experimentally.

The issue of endo/exo stereoselection should be discussed in terms of the four possible orientations of **3** with respect to the heterodiene. We have collectively denoted the interactions between heteroatoms of each moiety as head-to-head, leading to 6-cyano-substituted tetrahydropyridazines, and head-to-tail, which produces the 5-cyano-substituted derivatives. For each of these orientations, the cyano group can be in the endo or exo position. Overall, the four transition structures are **TS20** (exo), **TS21** (endo), **TS22** (exo), and **TS23** (endo) for head-to-head and head-to-tail approaches, respectively (Figure 5).

The calculated energy differences favor a head-to-head approach of the parent reactants (**TS20** and **TS21**), while **TS22** and **TS23** are significantly least stable. Thus, the azoalkene system **19** responds to the influence of the aromatic ring at N1 by stabilizing the transition structures leading to 6-cyano-substituted heterocycles. Data from Table 6 predict that the energy barrier for that regioselective pathway are  $\sim 1.9$  kcal/mol, in terms of zero-point energies ( $\Delta E_0^\ddagger$ ) and enthalpies ( $\Delta H^\ddagger$ ), lower in energy than the opposite formation of the 5-cyano-substituted regioisomers.

The endo/exo selectivity is almost negligible with respect to the head-to-tail approach but, for the alternative head-to-head cycloaddition, the difference in TS energy is 0.90 kcal/mol favoring the exo orientation which disagrees with the low exo/endo ratio found in the

**Table 6.** B3LYP/6-31G\* Energies and Activation Enthalpies (kcal/mol), and Activation Entropies (e.u.) for **TS20–TS23**

	$\Delta E^\ddagger$	$\Delta E_0^\ddagger$	$\Delta H^\ddagger$ <sup>a</sup>	$\Delta G^\ddagger$ <sup>a</sup>	$\Delta S^\ddagger$ <sup>a</sup>
<b>TS20</b>	+17.62	+19.34	+18.52	+32.24	-46.03
<b>TS21</b>	+18.63	+20.24	+19.44	+33.16	-46.01
<b>TS22</b>	+20.25	+22.10	+21.19	+35.08	-46.58
<b>TS23</b>	+20.27	+22.11	+21.19	+35.11	-46.71

<sup>a</sup> Computed at 298.15 K.

experiments. Sustmann et al.<sup>18</sup> have reported a theoretical study on the cycloaddition reactions of acrylonitrile with 1,3-butadiene or cyclopentadiene in which solvent effects are responsible for the reversion from the low exo preference in the gas-phase to an endo preference in solution, in agreement with the experiments. In that study, the endo transition states present higher dipole moments than the exo ones in the gas-phase, and the differences increase in solution due to the reorganization of electron distribution by the solvent. To evaluate solvent effects in the cycloaddition reactions of 1,2-diaza-1,3-butadienes and acrylonitrile, we have performed single point energy calculations at the B3LYP/6-31G\* level on the transition structures **TS20** and **TS21** with the polarized continuum model (PCM)<sup>19</sup> from the self-consistent reaction field (SCRFF)<sup>20</sup> methods implemented in Gaussian 98<sup>16</sup> in three different solvents with increasing polarity (benzene, dichloromethane, and acetonitrile).<sup>21</sup> As in the case reported by Sustmann et al., the endo transition structure (**TS21**) always presents a higher dipole moment and, at the same time, the energy

(18) Karcher, T.; Sicking, W.; Sauer, J.; Sustmann, R. *Tetrahedron Lett.* **1992**, *33*, 8027–8030.

(19) (a) Cancès, M. T.; Mennucci, V.; Tomasi, J. *J. Chem. Phys.* **1997**, *107*, 3032–3041. (b) Cossi, M.; Barone, V.; Cammi, R.; Tomasi, J. *Chem. Phys. Lett.* **1996**, *255*, 327–335. (c) Barone, V.; Cossi, M.; Tomasi, J. *J. Comput. Chem.* **1998**, *19*, 404–417.

(20) (a) Tomasi, J.; Persico, M. *Chem. Rev.* **1994**, *94*, 2027–2094. (b) Simkin, B.; Sheikhet, I. *Quantum Chemical and Statistical Theory of Solutions—A Computational Approach*; Ellis Horwood: London, 1995.

(21) The dielectric constant of acrylonitrile has been estimated to be  $\sim 38$  (*Kirk-Othmer Encyclopedia of Chemical Technology*, 3rd ed.; John Wiley and Sons: New York, 1980; Vol. 1, pp 414–426), and therefore reactions conducted in this medium should exhibit similar effects to those encountered in acetonitrile ( $\epsilon = 36.64$ ). For comparative purposes, our study has been restricted to the three solvents systems evaluated previously by Sustmann et al. (ref 18).

**Table 7. Electronic Energy Differences<sup>a</sup> (in kcal/mol) between Exo and Endo Transition Structures Together with Their Dipole Moments (in Debyes) in Different Polar Solvents**

medium	TS20 (exo)		TS21 (endo)	
	$\Delta\Delta E^\ddagger$	$\mu$	$\Delta\Delta E^\ddagger$	$\mu$
	CH <sub>3</sub> CN ( $\epsilon = 36.64$ )	0.00	4.56	+0.27
CH <sub>2</sub> Cl <sub>2</sub> ( $\epsilon = 8.93$ )	0.00	4.41	+0.42	4.82
C <sub>6</sub> H <sub>6</sub> ( $\epsilon = 2.247$ )	0.00	3.98	+0.88	4.31
gas-phase	0.00	3.59	+1.02	3.82

<sup>a</sup> Single point SCRF(PCM)/B3LYP/6-31G\*\*/B3LYP/6-31G\* energy calculations.

**Table 8. Bond Lengths (Å) and Bond Angles (deg) for TS20–TS23 at the B3LYP/6-31G\* Level**

	$d_{N1-C6}$	$d_{C4-C5}$	$\theta_{H-C5-C6-CN}^a$
TS20	2.523	2.058	160.89
TS21	2.542	2.063	-154.26
TS22	2.124	2.271	-151.49
TS23	2.130	2.259	156.73

<sup>a</sup> Hydrogen atom anti to the cyano group.

difference with respect to the exo one (TS20) diminishes (Table 7). The solvent effects on the exo/endo stereoselectivity are noticeable even in a solvent with a small dielectric constant (benzene). In all cases, the solvent disfavors the exo selectivity being responsible for the low stereoselectivity between the faces of the acrylonitrile found in the experiments.

Further estimations of bond distances and bond angles in the transition structures (Table 8) indicate that these correspond to concerted reactions. It should be noted that TS20 and TS21 exhibit a pronounced asynchronicity with a N1–C6 bond length close to 2.53 Å and a C4–C5 bond of 2.06 Å. As mentioned before, we have also calculated the transition structures emerging from **18** and **3**. Compared with TS20 and TS21, such structures have shorter N1–C6 distances (by 0.20 Å) and a slightly longer C4–C5 bond (by 0.13 Å). On the contrary, TS22 and TS23 are invariably more synchronous than their analogues devoid of phenyl group at N1.

In the latter computational study the absence of a discriminating substituent such as the bulky sugar moiety impedes an evaluation of the facial diastereoselection. Yet, we felt that it would be worthwhile to extend our studies by incorporating the complete chiral fragment so as to provide a more reliable model for the hetero-DA cycloaddition. This strategy, however, largely increases the computational expenditure and, accordingly, PM3<sup>22</sup> optimizations were performed on all the stationary points of the reaction coordinate leading to cycloadducts **4–7**. Because of the presence of the flexible sugar substituent, we have located the transition structures for each of the four diastereomeric approaches involving three possible conformations around the C4–C1' bond ( $\theta_{C3-C4-C1'-C2'}$ ). Only the most stable conformation for each diastereomeric transition structure is considered (Table 9). An in-depth conformational analysis has been included with the Supporting Information. Table 9 also outlines the energetics and the most salient geometric parameters for transition structures TS4–TS7 (Figure 6) corresponding to the endo and exo approaches to the *Re* and *Si* faces of the chiral azoalkene **1** (Scheme 2).

**Table 9. Heats of Formation (kcal/mol), Bond Lengths (Å), and Dihedral Angles (deg) for TS4–TS7**

	$\Delta H_f$	$d_{N1-C6}$	$d_{C4-C5}$	$\theta_{H-C5-C6-CN}^a$	$\theta_{C3-C4-C1'-C2'}$
TS4	-168.9	2.022	2.153	156	-171
TS5	-168.8	2.033	2.137	-146	-174
TS6	-168.3	2.015	2.162	-159	-43
TS7	-167.4	2.022	2.155	146	-42

<sup>a</sup> Hydrogen atom anti to the cyano group.

As can easily be deduced from bond lengths, these cycloadditions correspond to concerted highly synchronous processes. The TS6 and TS7, which involve the attack of **3** to the *Si* face of the heterodiene, exhibit shorter distances between N1 and C6, whereas TS4 and TS5 have in contrast relatively short distances between C4 and C5 atoms, these being the more synchronous structures. It should also be pointed out that an exo orientation of **3** diminishes the bond length between N1 and C6 (TS4 and TS6), whereas the endo orientation (TS5 and TS7) has shorter distances between C4 and C5. The dihedral angle defined by the carbon atom of CN and the axial proton at C5 (Hax-5–6–CN) reveals the lack of planarity experienced by C5 and C6 in the transition states. A greater pyramidalization is observed for transition structures with an endo orientation of the cyano group. Although the energy differences among transition structures are small, the enhanced stability of TS4 and TS5 suggests that the dienophile approaches preferentially to the *Re* face of the heterodiene following steric courses that can be denoted as  $[R(1)ReR(4)Re][Si]$  or  $[R(1)ReR(4)Re][Re]$ , respectively.<sup>23</sup> This stereoselection can doubtless be attributed to the steric factor determined by the acyclic carbohydrate at C4 of **1**. Nevertheless, calculation results allow us to expect a certain reactivity of **3** toward the *Si* face of **1** and, as a matter of fact, diastereomers **6** and **7** can be isolated in lower yield than that of **4** and **5**.

We have next studied the possible half-chair conformations adopted by each of these cycloadducts **4–7**. The conformation in which the cyano group is oriented axially will be thus labeled *ax*, whereas an equatorial arrangement will be denoted *eq*. The results are reported in Table 10.

Taking advantage of our previous X-ray crystallography and NMR studies which indicate a preferential axial orientation of the cyano group, one can expect that such an anomeric effect will be manifested by a rather short N1–C6 bond for the axial conformers. Indeed, the PM3 calculations evidence that hyperconjugative interaction even though for **4ax–7ax** the N1–C6 bond is 0.01 Å shorter than for **4eq–7eq**. Likewise, the axial conformers exhibit lower heats of formation than the equatorial ones. The energetic difference between axial and equatorial conformations should be related to the relative orientation of both the cyano group at C6 and the polyacetoxy fragment positioned at C4. For cycloadducts **4** and **6**, such groups exhibit a relative *trans* arrangement, and a conformation placing the cyano group in axial orientation will have the bulky carbohydrate moiety in an equatorial position. In both cases, that conformation is found to be more stable by >2.2 kcal/mol than the one with an equatorial cyano group. However, for cycloadducts **5** and **7**, the relative arrangement between both substituents

(22) Stewart, J. J. P. *J. Comput. Chem.* **1989**, *10*, 209–220 and 221–264.

(23) Avalos, M.; Babiano, R.; Cintas, P.; Jiménez, J. L.; Palacios, J. C. *Tetrahedron: Asymmetry* **1996**, *7*, 2333–2342.



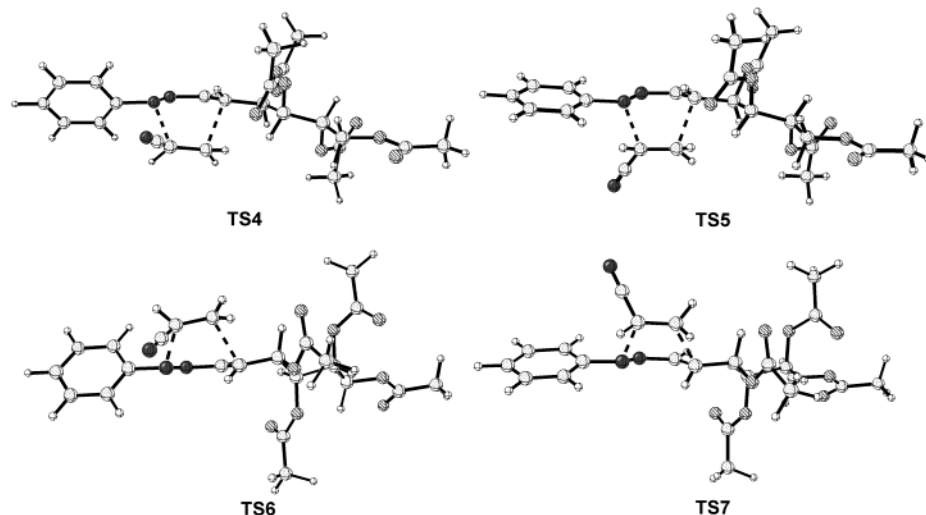


**Figure 6.** PM3 optimized transition structures for the hetero-DA cycloaddition of **1** and **3**.

**Table 10.** Energetics (kcal/mol) and Geometric Parameters (bond lengths in Å, dihedral angles in degrees) of Axial and Equatorial Conformers of the Cycloadducts **4–7** at the PM3 Level

	<b>4ax</b>	<b>4eq</b>	<b>5ax</b>	<b>5eq</b>	<b>6ax</b>	<b>6eq</b>	<b>7ax</b>	<b>7eq</b>
$\Delta H_f$	-236.2	-233.5	-235.3	-235.2	-234.6	-231.4	-231.0	-234.3
$\Delta H_r$	-31.0	-28.3	-30.1	-29.9	-29.4	-26.2	-25.8	-29.1
$d_{N1-C6}$	1.505	1.514	1.504	1.514	1.502	1.511	1.505	1.513
$d_{C4-C5}$	1.531	1.532	1.529	1.531	1.529	1.528	1.527	1.526
$\theta_{H-C5-C6-CN^a}$	170.3	56.1	-154.1	-62.6	-166.2	-61.1	135.7	63.7

<sup>a</sup> Hydrogen atom anti to the cyano group.

is cis and the presence of the cyano group in axial orientation causes a strong 1,3-diaxial congestion. Under these circumstances, the stabilizing anomeric effect still favors an axial conformation (**5ax** versus **5eq**) by only 0.2 kcal/mol; while in the case of **7**, the axial conformation (**7ax**) is 3.3 kcal/mol higher in energy than **7eq**. The additional penalty for the axial conformation owes its source not only to the 1,3-diaxial interaction, but also to the fact that the axial cyano group is very close to the acetoxy group located at the first stereocenter of the chiral chain. The values of the dihedral angle  $H_{ax-5-6-CN}$  equally reflect the preferred conformation of the heterocyclic ring. Thus, the corresponding dihedral angles for **4** and **6** are 170.3° and -166.2°, respectively, close to 180° (the expected value for a chair), whereas those of **5** and **7** are -154.1° and 135.7°, respectively. Therefore, it is not surprising that the cycloadducts **9** and **11** (the analogous counterparts of **5** and **7**, respectively) experience a spontaneous elimination of acetic acid that diminishes their steric hindrance.

### Conclusions

The hetero-Diels–Alder cycloaddition of chiral 1,2-diaza-1,3-butadienes, bearing a stereodiscriminating carbohydrate backbone, with acrylonitrile provides 6-cyano-substituted tetrahydropyridazines such as **4–7** or **8–11**. The transformation is found to be regiospecific without traces of the alternative 5-cyano-substituted derivatives, and it also exhibits a marked diastereoselection arising from a preferential attack to the *Re* face of the heterodiene. Moreover, the cyano group adopts an axial orientation that can be associated to a stabilizing anomeric effect.

DFT calculations at the B3LYP/6-31G\* level predict the observed regiochemistry and the exo/endo stereo-

selectivity, the latter being markedly influenced by solvent effects. The reason for having carried out further PM3 calculations concerns the possibility of studying the influence of the entire carbohydrate chain at a reduced computational cost. These results make it clear why a relative trans disposition between the sugar moiety and an axially oriented cyano group has a stabilizing effect. In contrast, a cis arrangement causes a severe 1,3-diaxial interaction, and the spontaneous elimination of acetic acid in such cycloadducts helps to relieve the steric congestion by virtue of forming an exocyclic double bond. Our results would appear to have broader implications concerning the stereocontrol of asymmetric cycloadditions, which will be addressed in future studies.

### Experimental Section

Melting points were determined on a capillary apparatus and are uncorrected. Microwave-irradiated reactions were performed on a monomode reactor<sup>24</sup> at a frequency of 2.45 GHz and up to 300 W of power. Solutions were evaporated under reduced pressure (15–30 mm) with a rotary evaporator, and the residue was flash-chromatographed<sup>25</sup> on a silica gel (400–230 mesh) column using diethyl ether–petroleum ether or benzene–diethyl ether mixtures as eluents. Optical rotations were measured at 22 °C using the wavelength at 589 nm (D line). <sup>1</sup>H and <sup>13</sup>C NMR spectra were recorded in CDCl<sub>3</sub> at 400 and 100 MHz, respectively. Chemical shifts are expressed in ppm downfield from the signal for internal TMS. FT-IR spectra were recorded on dry KBr pellets. UV spectra were measured with a double-beam spectrophotometer in the range of 200–500 nm and using a 1.0-cm cell. CD spectra were obtained between 190 and 350 nm in ethanol solutions. Mass spectra

(24) Loupy, A.; Petit, A.; Hamelin, J.; Texier-Boulet, F.; Jacquault, P.; Mathé, D. *Synthesis* **1998**, 1213–1234.

(25) Still, W. C.; Kahn, M.; Mitra, A. *J. Org. Chem.* **1978**, *43*, 2923–2925.

were determined at an ionizing voltage of 70 eV and an accelerating potential of 4 kV. Elemental analyses were recorded by the Servicio de Microanálisis (University of Extremadura).

The theoretical results presented in this work have been obtained using the Gaussian 98<sup>16</sup> series of programs. All the structures described were fully optimized by analytical gradient techniques and characterized by frequency calculations.

**General Procedure for the Preparation of 1,4,5,6-Tetrahydropyridazines 4–7 or 8–11 from the Reaction of 1,2-Diaza-1,3-butadienes 1 or 2 with Acrylonitrile 3.** A solution of (1*E*,3*E*)-4-(1',2',3',4'-tetra-*O*-acetyl-*D*-arabino-tetritol-1'-yl)-1-aryl-1,2-diaza-1,3-butadiene (**1** or **2**) (15 mmol) in acrylonitrile (20 mL) was subjected to microwave irradiation with temperature control (80–85 °C). TLC monitoring (benzene–diethyl ether 1:1) revealed, after 20 min, the appearance of four new products of *R*<sub>f</sub> 0.6 (**4** or **8**), 0.5 (**6** or **10**), 0.4 (**5** or **9**), and 0.3 (**7** or **11**). After 24 h, the excess of acrylonitrile was evaporated and compounds of *R*<sub>f</sub> 0.6, 0.4, and 0.3 were isolated by flash chromatography (diethyl ether–petroleum ether 1:1). Compound of *R*<sub>f</sub> 0.5 was isolated by preparative TLC (diethyl ether–petroleum ether 1:1) from a mixture containing compound of *R*<sub>f</sub> 0.6. Significant amounts of the starting diene were recovered: 1.50 g (24%) in the reaction of **1** with **3** or 1.89 g (28%) in the reaction of **2** with **3**.

**(4*R*,6*S*)-, (4*R*,6*R*)-, (4*S*,6*R*)-, and (4*S*,6*S*)-4-(1',2',3',4'-Tetra-*O*-acetyl-*D*-arabino-tetritol-1'-yl)-6-cyano-1-phenyl-1,4,5,6-tetrahydropyridazines (4–7).** Compound **4** was crystallized from diethyl ether (1.42 g, 26%) and had mp 167 °C, [α]<sub>D</sub> +123° (c 0.1, C<sub>6</sub>H<sub>6</sub>), λ<sub>max</sub> (96% aq ethanol) 206, 239, 265 nm (ε<sub>mM</sub> 12.3, 7.3, 12.3); IR (KBr) ν<sub>max</sub> 1745, 1610 cm<sup>-1</sup>; <sup>1</sup>H NMR (CDCl<sub>3</sub>) δ 7.35 (dd, *J* = 8.6 Hz, 7.5 Hz, 2H), 7.20 (d, *J* = 8.3 Hz, 2H), 7.04 (t, *J* = 7.5 Hz, 1H), 6.64 (bd, *J* = 1.4 Hz, 1H), 5.45 (dd, *J* = 9.1 Hz, 2.1 Hz, 1H), 5.25 (dd, *J* = 9.0 Hz, 2.2 Hz, 1H), 5.12 (ddd, *J* = 9.0 Hz, 4.4 Hz, 2.7 Hz, 1H), 4.88 (dd, *J* = 4.3 Hz, 2.9 Hz, 1H), 4.25 (dd, *J* = 12.7 Hz, 2.6 Hz, 1H), 4.16 (dd, *J* = 12.7 Hz, 4.5 Hz, 1H), 2.81 (m, 1H), 2.51 (m, 1H), 2.21 (s, 3H), 2.18 (s, 3H), 2.08 (s, 3H), 2.08 (s, 3H), 2.04 (ddd, *J* = 13.0 Hz, 13.0 Hz, 4.4 Hz, 1H); <sup>13</sup>C NMR (CDCl<sub>3</sub>) δ 170.5, 170.3, 170.0, 169.8, 145.0, 135.2, 129.3, 122.4, 116.5, 114.8, 70.3, 68.7, 67.9, 61.6, 43.9, 31.0, 24.8, 20.8, 20.6, 20.5. Anal. Calcd for C<sub>23</sub>H<sub>27</sub>N<sub>3</sub>O<sub>8</sub>: C, 58.34; H, 5.75; N, 8.87. Found: C, 58.23; H, 5.73; N, 8.81.

Compound **5**: yellowish oil (1.07 g, 21%), [α]<sub>D</sub> +87° (c 0.1, C<sub>6</sub>H<sub>6</sub>); <sup>1</sup>H NMR (CDCl<sub>3</sub>) δ 7.36 (dd, *J* = 8.1 Hz, 7.7 Hz, 2H), 7.23 (d, *J* = 8.4 Hz, 2H), 7.07 (t, *J* = 7.3 Hz, 1H), 6.84 (bs, 1H), 5.75 (bd, *J* = 8.6 Hz, 1H), 5.53 (bd, *J* = 9.5 Hz, 1H), 5.09 (ddd, *J* = 9.4 Hz, 3.2 Hz, 3.2 Hz, 1H), 4.82 (dd, *J* = 3.3 Hz, 3.3 Hz, 1H), 4.23 (d, *J* = 3.2 Hz, 2H), 2.50 (m, 1H), 2.39 (m, 2H), 2.18 (s, 3H), 2.16 (s, 3H), 2.08 (s, 3H), 2.07 (s, 3H); <sup>13</sup>C NMR (CDCl<sub>3</sub>) δ 170.7, 170.2, 170.1, 169.6, 145.4, 136.8, 129.2, 123.0, 116.7, 116.0, 70.1, 67.5, 67.4, 61.7, 41.7, 29.6, 24.8, 20.6, 20.4; HRMS calcd for C<sub>23</sub>H<sub>27</sub>N<sub>3</sub>O<sub>8</sub> 473.1798, found 473.1797.

Compound **6**: yellowish oil (0.21 g, 4%); [α]<sub>D</sub> -43° (c 0.1, C<sub>6</sub>H<sub>6</sub>); <sup>1</sup>H NMR (CDCl<sub>3</sub>) δ 7.35 (dd, *J* = 8.6 Hz, 7.5 Hz, 2H), 7.19 (d, *J* = 8.6 Hz, 2H), 7.05 (t, *J* = 7.5 Hz, 1H), 6.89 (bs, 1H), 5.55 (dd, *J* = 8.2 Hz, 3.2 Hz, 1H), 5.37 (dd, *J* = 6.9 Hz, 3.3 Hz, 1H), 5.15 (ddd, *J* = 11.1 Hz, 4.7 Hz, 2.9 Hz, 1H), 4.92 (dd, *J* = 4.1 Hz, 3.2 Hz, 1H), 4.26 (dd, *J* = 12.6 Hz, 2.7 Hz, 1H), 4.15 (dd, *J* = 12.6 Hz, 4.8 Hz, 1H), 2.96 (m, 1H), 2.36 (m, 1H), 2.28 (ddd, *J* = 12.3 Hz, 12.3 Hz, 4.4 Hz, 1H), 2.15 (s, 3H), 2.14 (s, 3H), 2.08 (s, 3H), 2.07 (s, 3H); <sup>13</sup>C NMR (CDCl<sub>3</sub>) δ 170.6, 170.0, 169.9, 169.8, 145.2, 135.9, 129.4, 122.6, 116.5, 115.2, 70.1, 68.3, 68.0, 61.5, 43.9, 31.9, 24.0, 20.8, 20.7; HRMS calcd for C<sub>23</sub>H<sub>27</sub>N<sub>3</sub>O<sub>8</sub> 473.1798, found 473.1805.

Compound **7**: yellowish oil (0.18 g, 3%), [α]<sub>D</sub> -89° (c 0.1, C<sub>6</sub>H<sub>6</sub>); <sup>1</sup>H NMR (C<sub>6</sub>D<sub>6</sub>) δ 7.26 (d, *J* = 7.8 Hz, 2H), 7.10 (bd, *J* = 2.5 Hz, 1H), 7.19 (dd, *J* = 8.6 Hz, 7.3 Hz, 2H), 6.91 (t, *J* = 7.1 Hz, 1H), 5.80 (dd, *J* = 7.0 Hz, 2.9 Hz, 1H), 5.63 (dd, *J* = 8.7 Hz, 2.8 Hz, 1H), 5.26 (ddd, *J* = 8.0 Hz, 5.0 Hz, 2.8 Hz, 1H), 4.26 (dd, *J* = 12.4 Hz, 2.8 Hz, 1H), 4.14 (dd, *J* = 12.5 Hz, 4.9 Hz, 1H), 3.87 (dd, *J* = 5.5 Hz, 3.1 Hz, 1H), 2.09 (m, 1H), 1.96 (m, 1H), 1.89 (s, 3H), 1.88 (s, 3H), 1.70 (s, 3H), 1.66 (s, 3H), 1.53 (ddd, *J* = 14.3 Hz, 8.6 Hz, 5.8 Hz, 1H); <sup>13</sup>C NMR (C<sub>6</sub>D<sub>6</sub>) δ 170.7, 170.6, 170.2, 147.1, 139.0, 130.0, 123.9, 117.6,

116.8, 70.8, 70.4, 69.1, 62.4, 43.0, 32.9, 25.1, 21.2, 20.9, 20.8. HRMS calcd for C<sub>23</sub>H<sub>27</sub>N<sub>3</sub>O<sub>8</sub> 473.1798, found 473.1799.

**(4*R*,6*S*)-, (4*R*,6*R*)-, (4*S*,6*R*)- and (4*S*,6*S*)-4-(1',2',3',4'-Tetra-*O*-acetyl-*D*-arabino-tetritol-1'-yl)-6-cyano-1-(4-methoxyphenyl)-1,4,5,6-tetrahydropyridazines (8–11).** Compound **8** was crystallized from diethyl ether (1.13 g, 21%) and had mp 123 °C, [α]<sub>D</sub> +191° (c 0.1, C<sub>6</sub>H<sub>6</sub>), λ<sub>max</sub> (96% aq ethanol) 204, 242, 270 nm (ε<sub>mM</sub> 11.7, 8.1, 9.3); IR (KBr) ν<sub>max</sub> 1744, 1611 cm<sup>-1</sup>; <sup>1</sup>H NMR (CDCl<sub>3</sub>) δ 7.13 (d, *J* = 9.0 Hz, 2H), 6.90 (d, *J* = 9.0 Hz, 2H), 6.63 (bs, 1H), 5.43 (dd, *J* = 9.1 Hz, 2.2 Hz, 1H), 5.24 (dd, *J* = 9.0 Hz, 2.2 Hz, 1H), 5.11 (ddd, *J* = 9.0 Hz, 4.5 Hz, 2.7 Hz, 1H), 4.76 (t, *J* = 3.8 Hz, 1H), 4.25 (dd, *J* = 12.7 Hz, 2.7 Hz, 1H), 4.15 (dd, *J* = 12.7 Hz, 4.6 Hz, 1H), 3.79 (s, 3H), 2.80 (m, 1H), 2.48 (m, 1H), 2.20 (s, 3H), 2.17 (s, 3H), 2.11 (ddd, *J* = 12.9 Hz, 12.9 Hz, 4.1 Hz, 1H), 2.08 (s, 3H), 2.07 (s, 3H); <sup>13</sup>C NMR (CDCl<sub>3</sub>) δ 170.5, 170.2, 170.0, 170.0, 155.7, 139.3, 135.3, 117.7, 116.5, 114.6, 70.4, 68.7, 67.9, 61.6, 55.5, 45.4, 30.8, 25.2, 20.8, 20.7, 20.5. Anal. Calcd for C<sub>24</sub>H<sub>29</sub>N<sub>3</sub>O<sub>9</sub>: C, 57.25; H, 5.81; N, 8.35. Found: C, 56.84; H, 5.96; N, 8.40.

Compound **9**: White solid from diethyl ether (0.98 g, 18%), mp 119 °C, [α]<sub>D</sub> +152° (c 0.1, C<sub>6</sub>H<sub>6</sub>); IR (KBr) ν<sub>max</sub> 1744, 1616 cm<sup>-1</sup>; <sup>1</sup>H NMR (CDCl<sub>3</sub>) δ 7.17 (d, *J* = 8.9 Hz, 2H), 6.90 (d, *J* = 8.9 Hz, 2H), 6.82 (d, *J* = 2.5 Hz, 1H), 5.68 (dd, *J* = 9.6 Hz, 1.1 Hz, 1H), 5.51 (dd, *J* = 9.4 Hz, 1.5 Hz, 1H), 5.08 (ddd, *J* = 9.3 Hz, 3.3 Hz, 3.3 Hz, 1H), 4.63 (t, *J* = 4.4 Hz, 1H), 4.23 (d, *J* = 3.2 Hz, 2H), 3.79 (s, 3H), 2.45 (dd, *J* = 4.5 Hz, 4.5 Hz, 2H), 2.38 (m, 1H), 2.18 (s, 3H), 2.16 (s, 3H), 2.08 (s, 6H); <sup>13</sup>C NMR (CDCl<sub>3</sub>) δ 170.6, 170.1, 170.0, 169.6, 156.3, 139.8, 137.3, 119.6, 116.8, 114.5, 70.3, 67.6, 67.6, 61.7, 55.5, 44.0, 29.8, 25.7, 20.7, 20.5. Anal. Calcd for C<sub>24</sub>H<sub>29</sub>N<sub>3</sub>O<sub>9</sub>: C, 57.25; H, 5.81; N, 8.35. Found: C, 57.25; H, 5.41; N, 8.55.

Compound **10**: yellowish oil (0.22 g, 4%), [α]<sub>D</sub> -98° (c 0.1, C<sub>6</sub>H<sub>6</sub>); <sup>1</sup>H NMR (CDCl<sub>3</sub>) δ 7.13 (d, *J* = 9.1 Hz, 2H), 6.90 (d, *J* = 9.0 Hz, 2H), 6.86 (bs, 1H), 5.55 (dd, *J* = 8.2 Hz, 3.3 Hz, 1H), 5.36 (dd, *J* = 6.9 Hz, 3.3 Hz, 1H), 5.14 (ddd, *J* = 7.9 Hz, 4.6 Hz, 2.7 Hz, 1H), 4.77 (t, *J* = 3.7 Hz, 1H), 4.26 (dd, *J* = 12.5 Hz, 2.7 Hz, 1H), 4.15 (dd, *J* = 12.7 Hz, 4.9 Hz, 1H), 3.80 (s, 3H), 2.94 (m, 1H), 2.34 (dd, *J* = 9.6 Hz, 3.5 Hz, 2H), 2.15 (s, 3H), 2.14 (s, 3H), 2.08 (s, 3H), 2.08 (s, 3H); <sup>13</sup>C NMR (CDCl<sub>3</sub>) δ 170.5, 170.0, 169.9, 169.8, 156.0, 139.5, 136.0, 118.4, 116.5, 114.6, 70.2, 68.3, 68.0, 61.5, 55.6, 45.8, 31.8, 24.4, 20.8, 20.7; HRMS calcd for C<sub>24</sub>H<sub>29</sub>N<sub>3</sub>O<sub>9</sub> 503.1904, found 503.1886.

Compound **11** was obtained as colorless crystals from diethyl ether (0.38 g, 7%) and had mp 150 °C (dec), [α]<sub>D</sub> -76° (c 0.1, C<sub>6</sub>H<sub>6</sub>); IR (KBr) ν<sub>max</sub> 1744, 1615 cm<sup>-1</sup>; <sup>1</sup>H NMR (CDCl<sub>3</sub>) δ 7.19 (d, *J* = 9.0 Hz, 2H), 7.06 (d, *J* = 2.0 Hz, 1H), 6.91 (d, *J* = 9.0 Hz, 2H), 5.63 (dd, *J* = 7.1 Hz, 2.9 Hz, 1H), 5.57 (dd, *J* = 8.4 Hz, 2.9 Hz, 1H), 5.07 (ddd, *J* = 8.8 Hz, 4.6 Hz, 2.8 Hz, 1H), 4.55 (t, *J* = 4.7, 1H), 4.27 (dd, *J* = 12.6 Hz, 2.8 Hz, 1H), 4.16 (dd, *J* = 12.7 Hz, 4.7 Hz, 1H), 3.80 (s, 3H), 2.55 (m, 1H), 2.43 (ddd, *J* = 14.0 Hz, 8.2 Hz, 5.2 Hz, 1H), 2.36 (ddd, *J* = 14.1 Hz, 4.1 Hz, 4.1 Hz, 1H), 2.17 (s, 3H), 2.15 (s, 3H), 2.08 (s, 3H), 2.07 (s, 3H); <sup>13</sup>C NMR (CDCl<sub>3</sub>) δ 170.6, 170.2, 170.1, 169.7, 156.7, 140.0, 138.6, 120.5, 116.1, 114.5, 70.0, 69.1, 68.2, 61.5, 55.5, 45.2, 32.0, 25.2, 20.7, 20.7. Anal. Calcd for C<sub>24</sub>H<sub>29</sub>N<sub>3</sub>O<sub>9</sub>: C, 57.25; H, 5.81; N, 8.35. Found: C, 56.99; H, 5.93; N, 8.39.

**(6*R*,4*Z*)-4-(2',3',4'-Tri-*O*-acetyl-1'-deoxy-*D*-erythritol-1'-ylidene)-6-cyano-1-(4-methoxyphenyl)-1,4,5,6-tetrahydropyridazine (16).** A solution of the (4*R*,6*R*)-1,4,5,6-tetrahydropyridazine **9** (150 mg, 0.30 mmol) in chloroform (3 mL) was stirred at room temperature. TLC monitoring (benzene–diethyl ether 1:1) revealed, after 2 h, the appearance of a new product of *R*<sub>f</sub> 0.5 (**16**). After 72 h, the solvent was evaporated and compound **16** was isolated as a yellowish oil by preparative TLC (diethyl ether–petroleum ether 1:1).

Compound **16**: yellowish oil (117 mg, 87%), [α]<sub>D</sub> -109° (c 0.5, CHCl<sub>3</sub>), λ<sub>max</sub> (96% aq ethanol) 201, 241, 327 nm (ε<sub>mM</sub> 34.1, 32.2, 18.1); <sup>1</sup>H NMR (CDCl<sub>3</sub>) δ 7.25 (bs, 1H), 7.20 (d, *J* = 8.9 Hz, 2H), 6.92 (d, *J* = 9.1 Hz, 2H), 5.67 (m, 2H), 5.23 (ddd, *J* = 9.8 Hz, 5.2 Hz, 5.2 Hz, 1H), 4.86 (dd, *J* = 5.3 Hz, 2.4 Hz, 1H), 4.29 (d, *J* = 4.8 Hz, 2H), 3.80 (s, 3H), 3.30 (bd, *J* = 16.4, 1H), 3.14 (dd, *J* = 16.4 Hz, 5.3 Hz, 1H), 2.12 (s, 3H), 2.09 (s, 3H), 2.07 (s, 3H); <sup>13</sup>C NMR (CDCl<sub>3</sub>) δ 170.5, 170.3, 169.7, 156.6, 139.9, 139.5, 127.2, 126.8, 120.0, 115.9, 114.6, 71.3, 67.8, 61.7,

55.5, 47.0, 28.3, 20.9, 20.7, 20.7; HRMS calcd for C<sub>22</sub>H<sub>25</sub>N<sub>3</sub>O<sub>7</sub> 443.1693, found 443.1697.

**Transformation of Cycloadducts 9 and 11 into Compounds 16 and 17.** (4*R*,6*R*)- or (4*S*,6*S*)-1,4,5,6-tetrahydropyridazines **9** or **11**, 0.075 g (0.15 mmol), were dissolved in chloroform (1 mL) in an NMR tube and allowed to stand at room temperature. Their quantitative transformation into compounds **16** or **17**, respectively, was monitored by <sup>1</sup>H NMR. After 4 days, no signals of the parent cycloadducts were detected in the <sup>1</sup>H NMR spectra.

NMR data of (6*S*,4*E*)-4-(2',3',4'-tri-*O*-acetyl-1'-deoxy-*D*-erythritol-1'-ylidene)-6-cyano-1-(4-methoxyphenyl)-1,4,5,6-tetrahydropyridazine (**17**): <sup>1</sup>H NMR (CDCl<sub>3</sub>) δ 7.28 (bs, 1H), 7.21 (d, *J* = 9.0 Hz, 2H), 6.92 (d, *J* = 9.1 Hz, 2H), 5.76 (bd, *J* = 9.3 Hz, 1H), 5.69 (dd, *J* = 9.4 Hz, 4.6 Hz, 1H), 5.21 (ddd, *J* = 6.0 Hz, 4.5 Hz, 1H), 4.87 (dd, *J* = 5.2 Hz, 2.0 Hz, 1H), 4.24 (m, 2H), 3.80 (s, 3H), 3.44 (bd, *J* = 15.7 Hz, 1H), 2.93 (ddd, *J* = 16.1 Hz, 5.2 Hz, 2.5 Hz, 1H), 2.10 (s, 3H), 2.09 (s, 3H), 2.07 (s, 3H);

<sup>13</sup>C NMR (CDCl<sub>3</sub>) δ 170.5, 170.1, 169.6, 156.6, 139.9, 139.4, 127.0, 126.5, 119.9, 115.3, 114.6, 71.5, 67.5, 61.6, 55.5, 46.7, 27.3, 20.8, 20.6.

**Acknowledgment.** This work has been supported by the Ministry of Science and Technology (Project BQU2000-0248) and the Junta de Extremadura-Fondo Social Europeo (Grants IPR00-C021 and IPR00-C047). R.G. wishes to acknowledge the Junta de Extremadura for a predoctoral fellowship.

**Supporting Information Available:** Conformational analysis (PM3 level of theory) for **TS4–TS7** and Cartesian coordinates of all the optimized structures with their computed total energies. This material is available free of charge via the Internet at <http://pubs.acs.org>.

JO016266L